Review

Wireless Monitoring of Biological Objects at Microwaves

IrinaVendik[1,*], Orest Vendik[1], Vladimir Pleskachev[2], Irina Munina[1], Pavel Turalchuk[1], and Vitalii Kirillov[1]

[1] St. Petersburg Electrotechnical University LETI,197376 St. Petersburg, Russia; ibvendik@rambler.ru (I.V.); ivmunina@etu.ru (I.M.); paturalchuk@etu.ru (P.T.); vvkirillov@etu.ru (V.K.)
[2] "SIMICON" Ltd., St.-Petersburg, Russia,vpleskachev@gmail.com (V.P.)
* Correspondence: ibvendik@rambler.ru

Abstract. Propagation of electromagnetic (EM) waves inside and on the surface of the human body is the subject of active research in area of biomedical applications. This research area is the basis for wireless monitoring of biological object parameters and characteristics. Much attention has been paid to radio-frequency identification systems, which are intended for biomedical applications. Solutions to the following problems are crucial to achieve the stated goals in the area of wireless monitoring: EM wave propagation inside regular and multilayer biological media, through the interface between different media, and on-body surface wave propagation. The biological object monitoring is based on a consideration of the followingprocesses: a) propagation of the EM wave in a biological medium considered as the dielectric with a high dielectric permittivity and substantial conductivity; b) penetration of the EM wave through the biological medium–air interface (wave reflection and refraction); c) propagation of the EM wave in a multi-layer biological medium; d) propagation of the EM wave along the plane or curved surface of biological objects.

Keywords: : electromagnetic waves, microwave frequency range, biological medium, wave propagation, reflection, refraction, surface wave, creeping wave, multilayered biological medium, body area networks

1. Introduction

Radio-frequency identification (RFID) systems are intended for biomedical applications, such as remote diagnostics of diseases, and for contactless monitoring and assessment of the human health. A great number of publications (monographs [**Error! Reference source not found.–Error! Reference source not found.**]), reviews in leading scientific journals, theses (dissertations) made in universities and scientific centers in many countries indicate great interest in this field of research. The following problems are of high importance: (i) propagation of electromagnetic (EM) waves inside biological media, (ii) propagation along interface between different media, (iii) on-body surface electromagnetic wave propagation, and (iv) RF system design for biological object monitoring.

Much attention has been paid in recent years to radio-frequency identification (RFID) systems, which are intended for biomedical applications, such as the remote diagnostics of diseases, contactless monitoring and assessment of the human health, and eventually for the provision of vital activity security. The RFID system, as a rule, consists of radio tags and readers with appropriate antennas and an information processing system. The peculiarities of the development of RFID tags for these applications are their miniature size and the ability to read information from the RFID tag taking into account

the properties of biological tissues considered as dielectrics with a high dielectric permittivity and significant losses of the EM signal.

Two types of RFID systems can be distinguished: near field and far field systems. For near field systems, magnetic coupling is used for radio tags and readers that eliminate the influence of the dielectric properties of the medium on the signal transmission. At the same time, for the RFID systems, the radiation of electromagnetic waves in the far zone is used providing a significant range of radio wave propagation when the radio tags are attached externally to clothing or directly to the body surface for use in emergency situations. In this case, the dielectric properties of the biological medium play a fundamental role.

Among health monitoring systems, wearable and implanted systems are widely used. In the former case, RFID tags are attached to clothes or to the human body surface. In the latter case, RFID tags are implanted into the human body. Figure 1 shows communication between wearable and implanted devices and an external base station [**Error! Reference source not found.**]

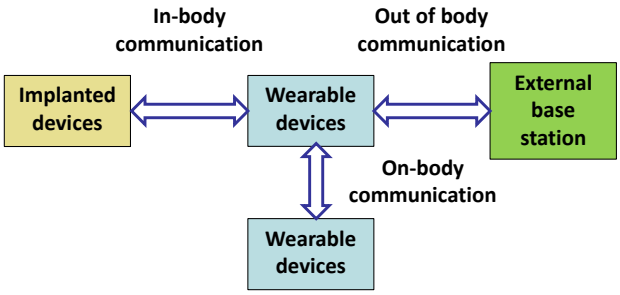

Figure 1. System for acquiring and transmitting information about the state of the human body. It includes implanted and/or wearable bioelectrical devices and an external base station receiving collected information.

Development of wearable wireless systems is highly challenged due to a wide spectrum of applications such as personal communication, medicine, firefighting, military, and radio frequency identification. Their light weight, low fabrication cost, easy manufacturing, and the availability of inexpensive materials make the wearable electronics very attractive. A new branch of wireless system technology is connected with the Wireless Body Area Network (WBAN). Such systems in combination with personal area networks provide monitoring of the state of biological systems (human body) in real time. For an adequate estimation and control of the data transfer of electromagnetic waves over the body surface it is necessary to describe properly the EM wave propagation.

Interface between the air and the body surface supports three basic EM wave modes: surface wave, leaky wave and creeping wave [**Error! Reference source not found.**]. The first two modes are well studied [**Error! Reference source not found.**, **Error! Reference source not found.**] while the latter [**Error! Reference source not found.**] exhibits a specific property on curved parts of the body and "creeping" into shadow regions [9, **Error! Reference source not found.**].

Solving the problem of the biological object monitoring, specific processes deserve specific consideration:

- Propagation of an EM wave in a biological medium (phase velocity and attenuation of the wave must be determined).
- Penetration of the EM wave through the biological medium–air interface; the process is characterized by the wave reflection and refraction.
- Propagation of the EM wave along the biological medium–air interface.

The processes listed are farther considered in detail.

2. Electromagnetic Waves in Biological Medium: Parameters and Characteristics

Bioelectrical devices placed inside or on the surface of the human body transfer information about the state of the body by means of EM waves and provide body – environment coupling, presenting information about processes in the body being observed in real time. Temperature and blood pressure sensors, a device analyzing the chemical composition of body fluids, etc., are examples of implanted devices. An implanted device introduces gathered data into a system that modulates the radiated EM wave and thereby provides data transfer to the environment. A wearable device may gather data for the state of the human body and/or transfer them to the environment or serve as an antenna coupled with an external base station. Coupling is provided largely by EM waves propagating inside the body. Propagation in the homogeneous tissue as well as in the layered medium is under consideration.

2.1. Propagation of the EM wave in a biological medium

The biological medium behaves as a dielectric material described by the dielectric permittivity and conductivity. The low frequency permittivity of the human biological tissue is high, since biological tissues consist of macromolecules, cells, and other components coupled by membranes. The membranes are of a high capacitance at low frequencies. Near 100 MHz, the capacitance of the membranes is governed by the rotation and vibration properties of polar molecules. These properties of water molecules are responsible for a high permittivity. A high dielectric loss is provided by a high conductivity of biological tissues. As a rule, the permittivity of the biological medium drops and its conductivity grows with frequency increasing [**Error! Reference source not found.**].

The most common models used to describe the electrical behavior of tissues are: Debye, Cole-Cole, and Cole-Davidson models [11].

The frequency dependence of the permittivity can be analytically described by the following formula [12]:

$$\varepsilon(\omega) = \varepsilon_\infty + \frac{\varepsilon_s - \varepsilon_\infty}{\left[1+(i\omega\tau)^{1-\alpha}\right]^\beta} + \frac{\sigma_s}{i\omega\varepsilon_0} = \varepsilon'(\omega) + i\varepsilon''(\omega) \quad (1)$$

Here ω is the angular frequency of the electric field, ε_∞ is the dielectric permittivity at the frequency $\omega\to\infty$, caused by electron polarizability, ε_s is the static (low-frequency) permittivity, σ_s is the static conductivity, determined by the motion of charged particles, ε_0 is the free space permittivity, τ is the characteristic relaxation time of the medium, determined as the time required for molecules or dipoles to return to their original state, which was disturbed by the applied electric field. For $\alpha = 0$ and $\beta = 1$, the equation (1) corresponds to the Debye model. For $0 < \alpha < 1$ and $\beta = 1$, the equation is consistent with the Cole-Cole model, which takes into account the dispersion of the relaxation time. For $\alpha = 0$ and $0 < \beta < 1$, the equation corresponds to the Cole-Davidson model, which is characterized by an asymmetric distribution of relaxation time. Biological tissue is usually described by the Debye model, less by the Cole-Cole model.

Fractional terms in (1) indicate the relaxation (non-resonance) type of the frequency dependent permittivity, which has a real and an imaginary part. Together with the imaginary part of the permittivity, the electrical conductivity of the medium $\sigma = \varepsilon_0\varepsilon''\omega + \sigma_0$ is used (σ_0 is the frequency-independent conductivity). The frequency dependence of the real and imaginary parts of the permittivity and conductivity calculated for an averaged biological tissue by formula (1) is given in Fig. 2 [13].

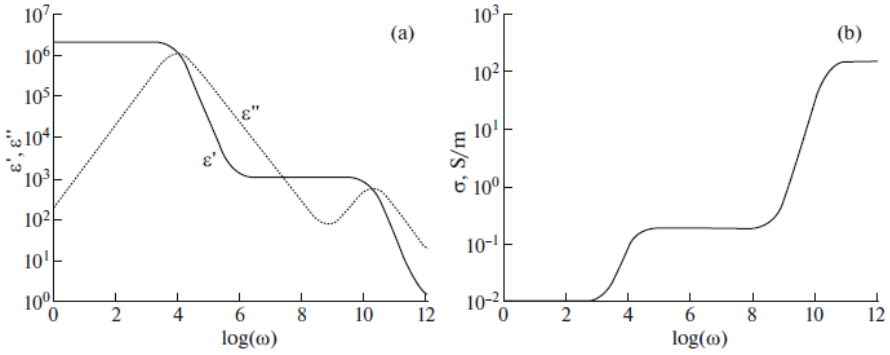

(a) **(b)**

Figure 2. Frequency dependence of the real and imaginary parts of the dielectric permittivity (a) and conductivity (b) calculated for a biological tissue by the Debye formula.

The dielectric properties of biological tissues were measured an analyzed in a wide frequency range (10 Hz – 20GHz) in [14, 15]. The measurements were carried out in-vitro on different tissue samples extracted from a living organism under fixed external conditions. Further studies showed that there is a significant scattering in the results of measurements of the parameters of biological tissues. The spread is due to the use of various measuring techniques, as well as the sensitivity of tissues to changes in temperature, humidity, etc. In [16, 17] parameter scattering was analyzed. Parameters of various tissues in the frequency range 2-10 GHz are presented in Table 1.

Table 1. Electric properties of different biological tissues.

Tissue	Dielectric permittivity	Conductivity, S/m
Skin	28-46	1.00
Muscle	29-70	0.90-1.55
Tendon	46.5	1.10
Fat	2-6	0.05
Cortical bone	12	0.20
Trabecular bone	12.5-27	0.44-0.55

The propagation of EM waves is described by the Maxwell equations. The solution for the E component of a plane harmonic wave propagating in the z direction has the form:

$$E(z) = E_m e^{-ikz} e^{i\omega t} \tag{2}$$

Here, factors $e^{-\alpha z}$ and $e^{-i\beta z}$ describe, respectively, the attenuation and the phase advance of the wave, and factor $e^{i\omega t}$ describes the harmonic dependence of the wave phase on time.

In general case, the propagation of an EM wave is characterized by the complex wave number:

$$k(\omega) = \beta(\omega) - i\alpha(\omega). \tag{3}$$

Here β is the propagation constant and α is the damping ratio:

$$\beta(\omega) = \omega\sqrt{\varepsilon_0 \varepsilon'(\omega)\mu_0}\,, \tag{4}$$

$$\alpha(\omega) = \frac{\sigma(\omega)}{2}\sqrt{\frac{\mu_0}{\varepsilon_0 \varepsilon'(\omega)}} \tag{5}$$

Let us take into account that the biological medium is isotropic and the magnetic permeability of the medium is equal to the permeability of the free space μ_0.

The phase velocity of the wave is determined by the propagation constant β:

$$v_{ph}(\omega) = \omega / \beta(\omega) \tag{6}$$

2.1. Propagation of the EM wave through the biological medium–air interface: reflection and refraction

Let us consider a source of EM wave designed as a small-size antenna implanted into the biological tissue. Unlike the simple case of wave propagation in a homogeneous isotropic medium, the propagation of an EM wave through the biological tissue–free space (air) interface brings up a number of specific problems [18]-[19].

A segment of the wave that is much smaller than the distance to the source position can be roughly considered as a plane wave (Figure 3 (a)). Hence, the propagation of spherical EM waves that are obliquely incident on the interface between two insulators far away from the source can be described in terms of plane waves.

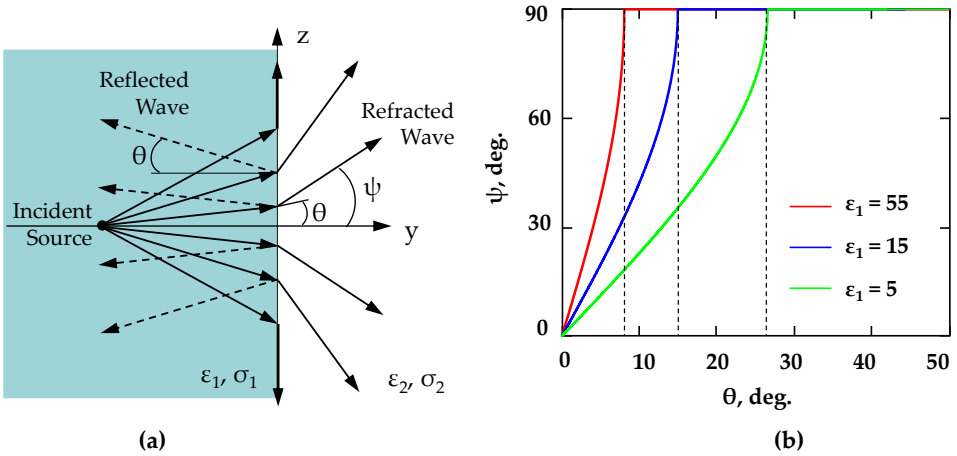

Figure 3. The spherical wave propagation across the interface between two dielectrics (a) and the dependence of the angle of refraction on the angle of incidence (b) the dielectrics with different values of permittivity (ε_1 = 55, 15, 5) and the free space.

The diffraction of a spherical wave on a flat interface between two media (Figure 3 (a)) is characterized by the refraction angle ψ of a plane EM wave related to the angle of incidence θ as

$$\cos(\psi) = \sqrt{1 - \frac{\varepsilon_1}{\varepsilon_2}\sin^2(\theta)}\,. \tag{7}$$

For ε_1 = 55 (biological medium (muscle) at frequency of 2.45 GHz), and ε_2 = 1 (air), the deviation of the incident wave from the normal to the interface by more than 7.75° causes the deviation of the refracted wave from the normal by 90°. That means that the refracted wave does not propagate in the medium with ε_2 = 1 (Fig. 3 b). The angle of incidence θ_0 at which the refracted wave cannot propagate in the environment is called the angle of total internal reflection. Only a small fraction of the power flux emitted by the radiator lying in the sector of ±7.7º enters the free space, whereas the most of the radiated energy is transformed into a surface wave at the interface, which is absorbed at the boundary. The higher dielectric contrast at the interface, the smaller portion of the radiated energy is able to penetrate into the air.

2.3. Propagation of the EM wave through the interface of biological tissue and free space.

In case of using a device (sensor) implanted in the biological medium, a degradation of the electromagnetic signal is of high importance. The high loss factor leads to attenuation of a signal in the medium. Additionally, a high contrast of the dielectric permittivity of the biological medium and the free space, results in a strong wave reflection from the interface. It is important to study the EM wave propagation in biological medium, including the refraction of waves at the biological tissue–free space interface.

Generally, for electromagnetic waves propagating toward the interface between the different dielectric media, the effects of reflection and refraction occur at the interface.Taking into account the dielectric loss in the biological tissue, the attenuation of the

wave caused by the refraction of the wave propagating through the boundary between two dielectrics [13, 18, 19] is defined as

$$A_{refr} = -10\log\left(\frac{P_2}{P_\Sigma}e^{-\alpha h}\right). \quad (8)$$

Here α is the attenuation coefficient determined by (5), h is the distance from the source to the boundary between two media, P_Σ is the total power radiated by the antenna implanted in the biological medium and defined as

$$P_\Sigma = 30I_0^2\int_0^{\frac{\pi}{2}}(\cos\theta)^2\sin\theta d\theta \quad (9)$$

P_2 is the power radiated by the antenna into the free space:

$$P_2 = 30I_0^2\int_0^{\theta_0}(\cos\theta)^2\sin\theta d\theta \quad (10)$$

where I_0 is the current amplitude, $Z_1 = \sqrt{\frac{\mu_0\mu_1}{\varepsilon_0\varepsilon_1}}$ is the wave impedance of the medium containing the radiator.

Scattering parameters between the miniaturized antenna inside the homogeneous tissue and the external patch antenna located outside the tissue were simulated with the use of full wave electromagnetic simulator SEMCAD X by SPEAG [24]. The transmission coefficient for typical structure containing an implanted dipole with the 50 Ohm impedance at the frequency of 915 MHz is estimated for the following dielectric parameters of the homogeneous tissue: the dielectric permittivity $\varepsilon_1 = 55$ and the electric conductivity $\sigma_1 = 1.08$ S/m.

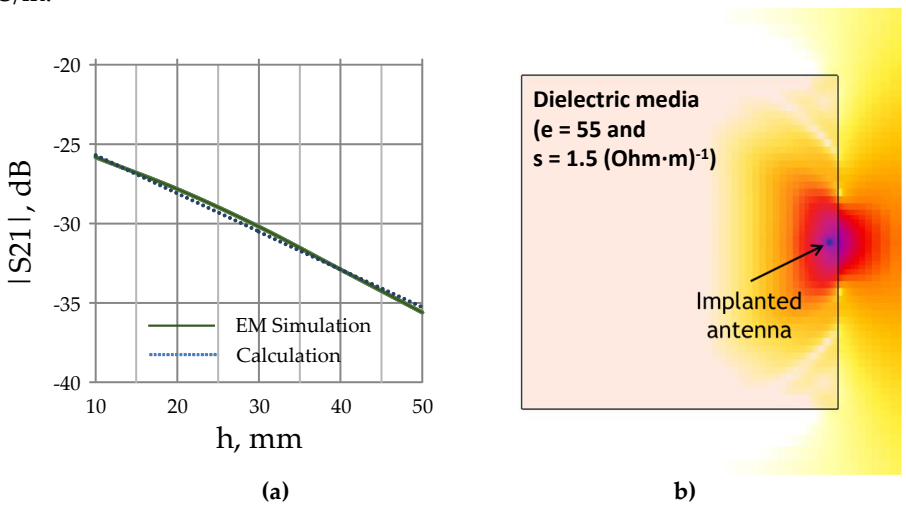

(a) **b)**

Figure 4. Transmission coefficient module versus distance between the implanted dipole and the tissue surface (a). The electric field distribution radiated by antenna inside the dielectric media (b)

Simulated transmission coefficient module between the implanted antenna in the homogeneous tissue and the receiver located outside is shown in Figure 4. The results of electromagnetic simulations are agreed well with the results of the analytical consideration described by equation (8). In order to verify the simulations results, the implanted antenna optimized for 915 MHz has been fabricated and embedded inside the liquid with dielectric properties being equivalent to the biological tissue. The scheme of the experimental setup used for measuring response of the implanted antenna is shown in Figure 5.

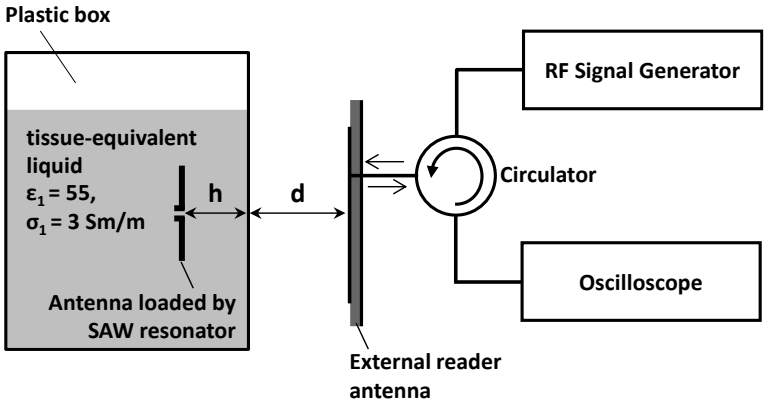

Figure 5. Scheme of the experimental setup for measuring response of the implanted antenna loaded by the SAW sensor.

The measured return loss of the fabricated dipole embedded into the plastic box filled with the solution of sodium chloride and Ethanol with dielectric properties similar to the properties of a biological medium is shown in Figure 6.

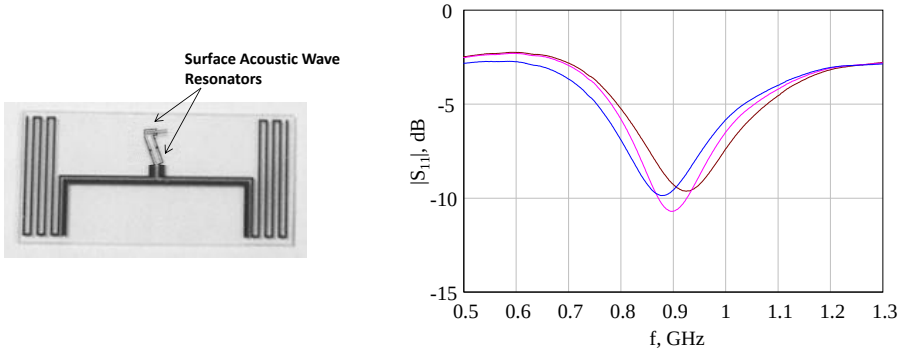

(a) **(b)**

Figure 6.(a) Design of the implanted dipole loaded by SAW resonator; (b) return loss measured for three test samples of implanted dipole in the tissue-equivalent liquid.

The measured dielectric permittivity and the conductivity are $\varepsilon_r = 55$ and $\sigma = 3$ S/m, respectively. The dipole was fabricated using the direct photolithography process on the quartz substrate. The surface of the substrate with 0.5 mm of thickness was covered by plating layer of copper (4 μm) using chromium sub-layer and then photolithography and etching were carried out.

Experimental study of the link attenuation between the patch antenna and the implanted sensor based on the fabricated dipole loaded by the SAW (surface acoustic wave) resonator was performed. The SAW resonator implemented with the 50 Ohms output impedance is connected directly with the antenna terminals by gold wires. The tag based on SAW element is the temperature dependent sensor used for wireless measurements. The tag was embedded inside the liquid equivalent of the biological tissue. The RF analog signal generator Agilent N5181A with signal power level of 23 dBm was used to interrogate implanted antenna. The backscattered response of the antenna was registered by the oscilloscope Agilent Technologies Infiniium DSO80304B. The SAW sensor response has been observed at the resonant frequency 907 MHz. The backscattered response power level of the dipole antenna with the SAW sensor as a function of the distance between the patch antenna and the tissue-equivalent liquid box surface d and of the distance between the implanted sensor and the tissue surface h are shown in Figure 7.

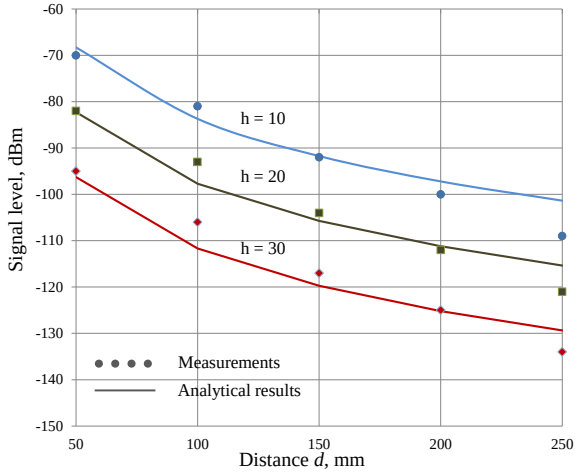

Figure 7. Measured signal power level versus distance between the patch antenna and the tissue-equivalent liquid d for different distance h between the implanted dipole and the tissue surface h.The results of calculation by (11) are presented by solid lines and the measured results are shown by dotes.

The power level of the backscattered signal received by antenna (P_R) shown in Figure 7 (solid lines) is evaluated using the following equation:

$$P_R = 2\left(-A_{refr} + PL + IL\right) + IL_{SAW} + P_T. \quad (11)$$

Here A_{refr} is calculated using (8), PL is the path loss between the radiator embedded inside the homogeneous tissue and the external antenna located outside the tissue at the distance d, IL corresponds to the insertion loss caused by the loss in cables of the experimental setup and antenna mismatching, IL_{SAW} is the SAW resonator loss, P_T is the power level of the transmitted signal. The following parameters in (11) were used: IL = 10 dB, IL_{SAW} = 15 dB, P_T = 23 dBm. The dielectric permittivity ε_1 = 55 and the conductivity σ_1 = 3 S/m for the tissue-equivalent liquid.

Evidently, the EM wave is remarkably reflected and refracted on the boundary between the biological tissue and the air. The power level decreasing in the plane of reader antenna is observed by using implanted sensors. From this point of view, the on-body location of RFID components is preferable.

2.4. Estimation of EM Waves Attenuation by Using Matching Layer

Due to a strong attenuation of EM signal propagating through the biological media it is interesting to analyze a possibility to increase transmission coefficient between the implanted antenna and antenna of the reader. Firstly, let us consider the propagation between two dipole antennas one of which is placed in bio-tissue. For modeling the biological tissue properties, the frequency dependent model of muscle was used exhibiting relative permittivity 54 and electric conductivity 0.94 S/m at 0.915 GHz., where h is the distance between the surface of the tissue and implanted antenna and d is the distance between the surface of the tissue and antenna of the reader. The results of electromagnetic simulation of the system (for h= 10 mm, d= 50 mm) obtained by FDTD method using full-wave electromagnetic simulator SEMCAD X by SPEAG [24]. As a result, the signal attenuation between antennas is 26 dB.

Using a special matching layer placed at the tissue/air interface leads to decreasing of reflection coefficient of EM wave from the interface. The dielectric constant of the matching layer depends on dielectric permittivity of matched media and can be calculated by the following formula:

$$\varepsilon_{tr} = \sqrt{\varepsilon_{bio}\varepsilon_{air}}, \quad (12)$$

Where ε_{bio} and ε_{air} are the dielectric permittivity of bio-tissue and free space correspondingly, ε_{tr} is the dielectric permittivity of the matching layer. The thickness of layer is equal

to quarter of the wavelength guided in the matching layer at the operational frequency of the antennas.

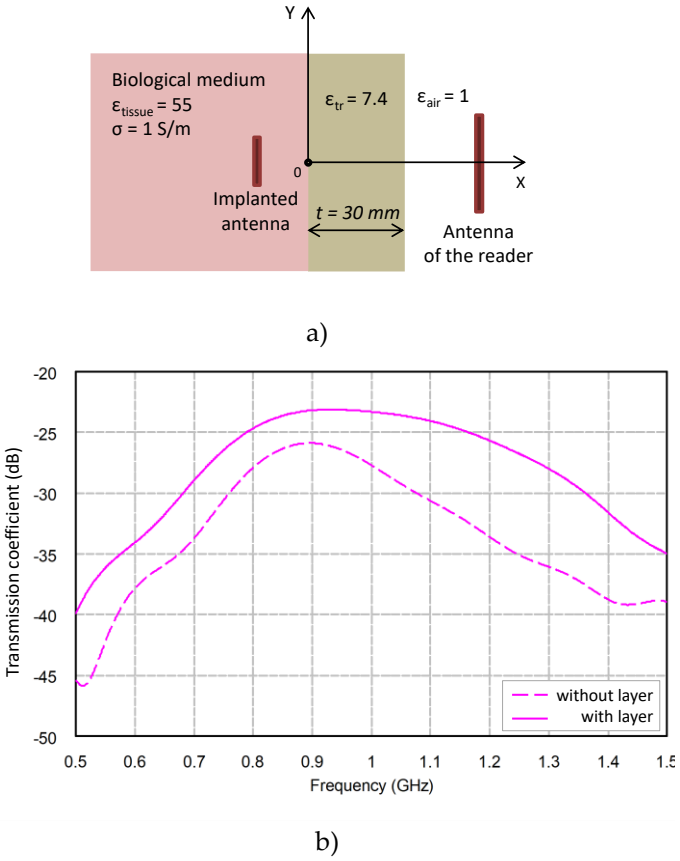

Figure 8. Implanted antenna with matching layer placed between the biological tissue and antenna of the reader (a) and the transmission coefficient between the antennas (solid line – with matching layer, dashed line – without it) (b).

The results of modeling of the system with two antennas including the matching layer are shown in Fig. 8. At 0.915 GHz, the thickness of the layer is equal to 30 mm and the dielectric permittivity ε_{tr} = 7.34. In accordance with the results of electromagnetic simulation, the presence of the matching layer allows improving S_{21} up to 3 dB. The E-field distribution along X-axis is shown in Fig. 9. It can be concluded that using matching layer noticeably improves the transmission coefficient from -26 dB to -23 dB at the operational frequency. However, the disadvantage of such approach is necessity of using and fixing an additional object on a human body. Though it is promising in case when the implanted antenna is placed deep inside the body and signal strongly attenuates in the biological medium.

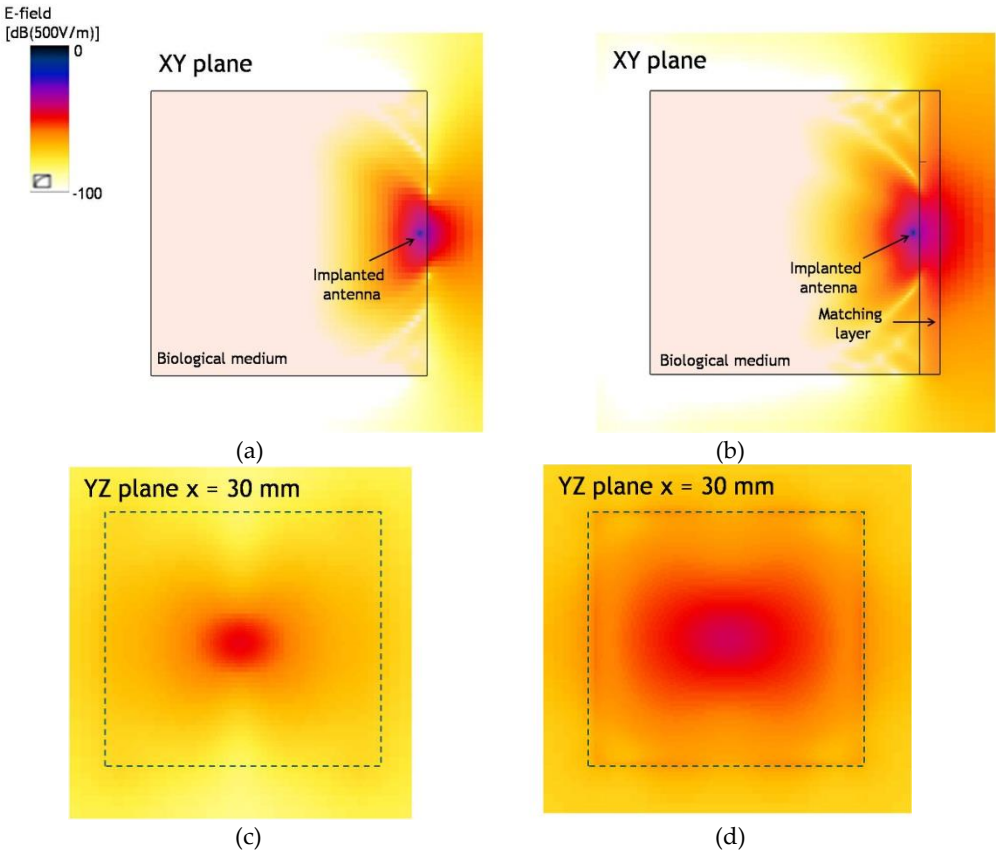

Figure 9.E-field distribution: XY plane without (a) and with matching layer (b) and YZ plane at distance 30 mm from tissue without (c) and with (d) matching layer.

2.5. Propagation of the EM wave in a multi-layer biological medium

Propagation of the electromagnetic waves over the surface and through the internal tissues of the human body is the subject of extensive research that bridges the electrodynamics and medical science. This area of research lays the foundation for non-invasive biological object monitoring [13]. In contrast with the widespread X-ray diagnostic method, low-power microwave radiation is harmless for the human body if adequately safe microwave signal power level is applied. Electromagnetic wave propagation through the various human tissues is the subject of the research which helps to detect early signs of disease and to diagnose the degree of tissue damage. The matter is complicated by the fact that the different parts of the human body contain many tissue layers with individual dielectric properties and the geometry specific to a particular person. Hence the research goal is the in-vivo estimation of the particular tissue state inside the multilayered human tissue structure. The trabecular bone tissue which is replaced by the marrow bone tissue when a patient is diseased with osteoporosis is the object of the research.

Microwave imaging techniques and many other applications are utilized for extracting the tissue model parameters and registering harmful changes in the tissue condition due to the microwaves being able to penetrate inside human tissues. The scattered or reflected signals from those tissues are measured and processed giving useful insight on the underlying tissue structure. The principle of microwave imaging system operation is based on observable contrast in the electrical properties between various parts of the imaged objects and their surroundings. The microwave imaging technique is used for the examination of different tissues and organs of a patient: imaging of breast cancer [25 -26], brain stroke diagnostics [27-29], microwave bone imaging [30-35], etc. In all cases mentioned, the multi-layer dielectric medium is investigated. It is important to analyze multiple reflections and refraction for many layer boundaries. Additionally, the EM wave attenuates in each layer depending on the conductivity, which is high enough for all tissues in the human body. The main problem in the in-vivo analysis of the tissue is a low

energy level of the EM wave reaching a target tissue and, as the result, weak response signal making it difficult to obtain a reliable observation.

Consider the EM wave propagating in the multilayered dielectric medium. As an example, a finger of the human hand is taken as the multilayered object composed of different tissues. The finger contains skin, fat, muscle, bone etc. Bone mineralization level may be used as an estimation of the bone condition of the bone suffering from the osteoporosis. The dielectric permittivity of the bone depends on the degree of bone damage, therefore measurement results of the bone dielectric permittivity may be used as a diagnostic criterion estimating osteoporosis severity. The advantage of performing measurements on the finger is that the finger bones are covered by thin layers of skin, fat, and muscle tissues and therefore the trabecular bone tissue is more accessible to the EM waves.

A simplified model of the finger containing two phalanges is presented in Figure 10. This model is used to simulate EM wave propagation through the finger. The dimensions of the model components were chosen in accordance with the average length, width, and height of the distal and middle phalanges of the "average human" index finger. Two EM wave excitation probes were used to perform simulations: open-end coaxial [14, 15, 36-38] (Figure 11) and a microstrip antenna [32-33] printed on a dielectric substrate which was applied on the finger (Figure 12 (a)).

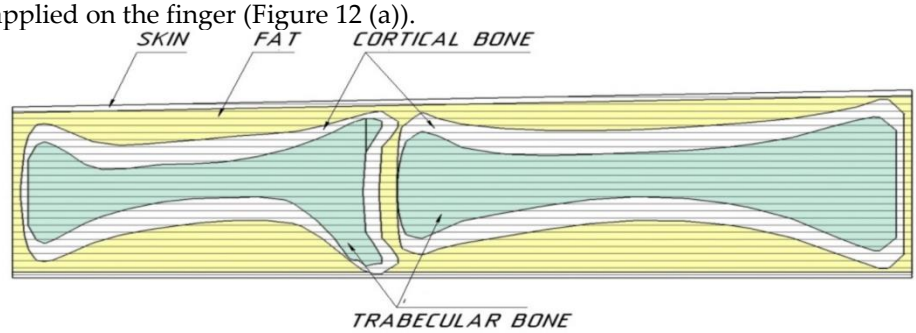

Figure 10. Finger model cross-section.

The electric field distribution in case of using open-end coaxial probe, obtained by full-wave simulation [39], is presented in Figure 11. Only a tiny fraction of the EM wave energy penetrates into the bone tissue due to intensive reflection and remarkable attenuation in the surrounding tissues.

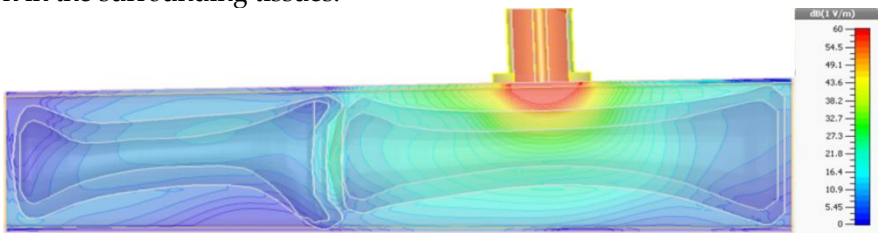

Figure 11. Electric field distribution within the finger volume excited by the open-ended coaxial probe.

EM wave penetrates in the finger much more effectively if the finger is placed between a planar antenna and a reflecting surface made of perfect conducting material (Figure 12 (a)). In this case two resonances are observed in the frequency range 10 MHz – 5 GHz. The resonance response of the finger placed between the antenna and reflecting plane is well pronounced: the wave excited inside the finger volume exists in the form of many different modes as shown in Figure 12 (b) and 12 (c). It is important that in the resonant structures the electric field penetrates inside the trabecular bone deeper than the field excited by the coaxial probe.

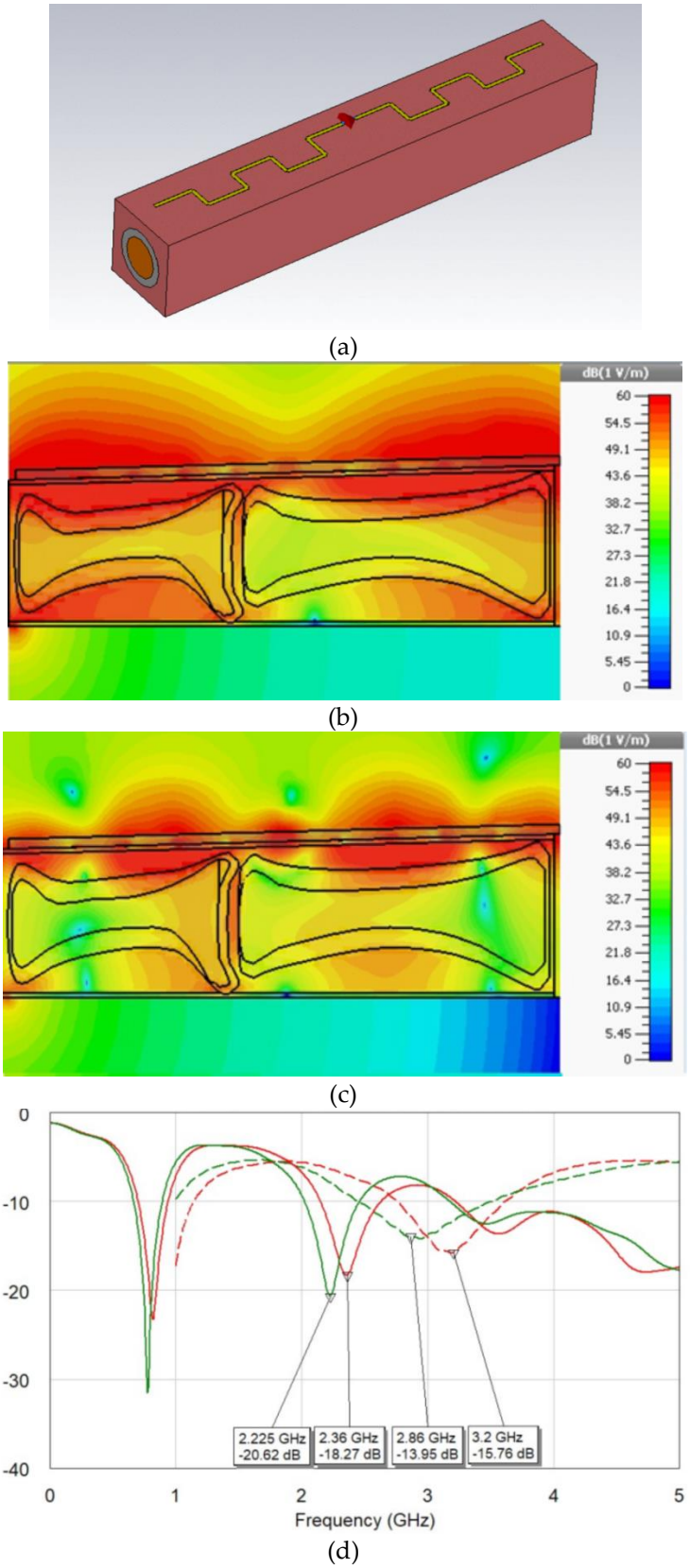

Figure 12. Electric field distribution in the finger placed between the planar antenna on the top and the reflecting surface on the bottom: (a) printed antenna applied on the finger, (b) electric field distribution within the finger at 750 MHz, (c) electric field distribution within the finger at 2225 MHz, and (d) return loss of the antenna: red curves – diseased bone, green curves – healthy bone, solid lines – modeling, dashed lines - experiment.

The printed antenna was manufactured and tested on two persons one of them is healthy and the other has confirmed osteoporosis. Both EM field mode frequencies revealed in the experiment with the printed antenna applied on the finger are close enough to the modeling results as shown in Figure 12 (d) despite the frequency shift around 600 MHz which can be explained by the difference in tissue permittivity in modeling and real life. The mode at the frequency f = 750 MHz is marginally sensitive to variations in dielectric permittivity of the trabecular bone whereas the mode with higher frequency at 2225 MHz (2860 MHz in experiment) shifts by about 140 MHz (340 MHz in experiment) for the healthy and diseased persons. This fact could be used to predict osteoporosis. If the measurements are being performed regularly on a particular patient, the measured resonance frequency on the trabecular bone condition is obtained in dynamics. This systematic approach makes the measurements unsusceptible to the absolute value of the resonant frequency which depends on finger geometry, individual tissue properties etc. as the measurement dynamics brings the personalized results for a particular patient.

3. Propagation of an EM wave along the surface of biological objects

The interface between two dielectric media with different values of permittivity (body surface and air) generates waves propagating along it. The interface between the air and the body surface supports three basic EM wave modes [**Error! Reference source not found.**]: surface wave (SW), leaky wave (LW) and creeping wave (CW). The first two modes are well studied [**Error! Reference source not found.**, **Error! Reference source not found.**] while the latter [**Error! Reference source not found.**, **Error! Reference source not found.**, **Error! Reference source not found.**] exhibits a specific property of rounding curved parts of the body and "creeping" into shadow regions.

This property of the CW is of high importance for the body networks making non line-of-sight communications possible. Analytical study of the CW properties is presented in [**Error! Reference source not found.**, **Error! Reference source not found.**, **Error! Reference source not found.**, **Error! Reference source not found.**] as applied to wave propagation over an uniform cylinder.

SW represents directed EM radiation localized near the interface and propagating along the interface surface. SW rapidly attenuates propagating away from the interface in the direction normal to the interface. LW is radiated at some angle to the interface defined by the permittivity ratio of bordering insulators. Finally, CW arising in case of the curved interface propagates along the curved surface and can envelope the surface, falling into a shadow area (Figure 13).

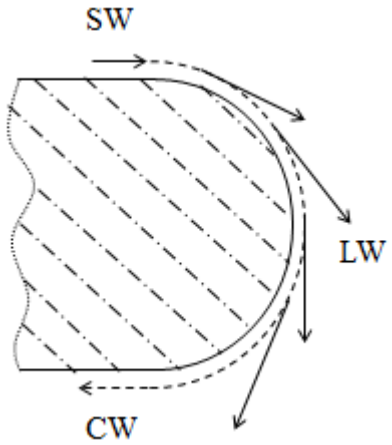

Figure 13. Types of waves on a surface with a complex shape.

Let us consider EM wave propagating over plane and curved surfaces of a human body [**Error! Reference source not found.**, **Error! Reference source not found.**, **Error! Reference source not found.**]. For modeling the wave propagation process, it is necessary to use a phantom of a human body. Wide variety of human body forms and sizes

challenges a procedure of description in a form suitable for numerical simulations. Simplification of a digital human body phantom geometry is necessary to speed up computations and compare the results with analytical models. Let us consider the phantom in the form of cylinder made of uniform lossy dielectric or perfect conducting material with a simple geometric form in a lateral cross section [**Error! Reference source not found.**, **Error! Reference source not found.**, **Error! Reference source not found.**]. The phantom made of lossy dielectric with $\varepsilon_r = 42.6$ and $\sigma = 1.66$ S/m is shown in Figure 14. It is formed by the rectangular box combined with a half-cylinder with radius r. The box represents human chest and back with a flat surface and the cylinder models the forearm and shoulder. The phantom dimensions correspond to averaged human dimensions. The structure in Figure 14 contains the phantom itself and the disk antenna providing the surface wave excitation. The field computation path is shown in Figure 14 (b) by blue line, which goes along the shoulder and further along the back surface. The surface wave field distribution is simulated over the flat surface while the CW distribution is kept on the cylindrical surface.

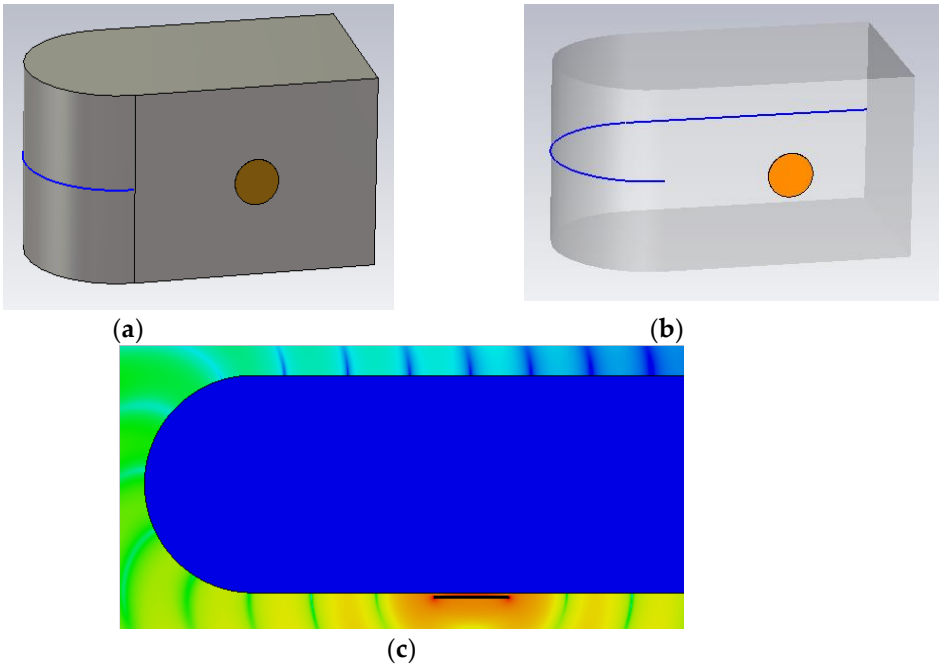

Figure 14. Phantom for the surface and creeping wave modeling: (**a**) Front sight; (**b**) Translucent view with field computation path (blue curve); (**c**) Electric field distribution.

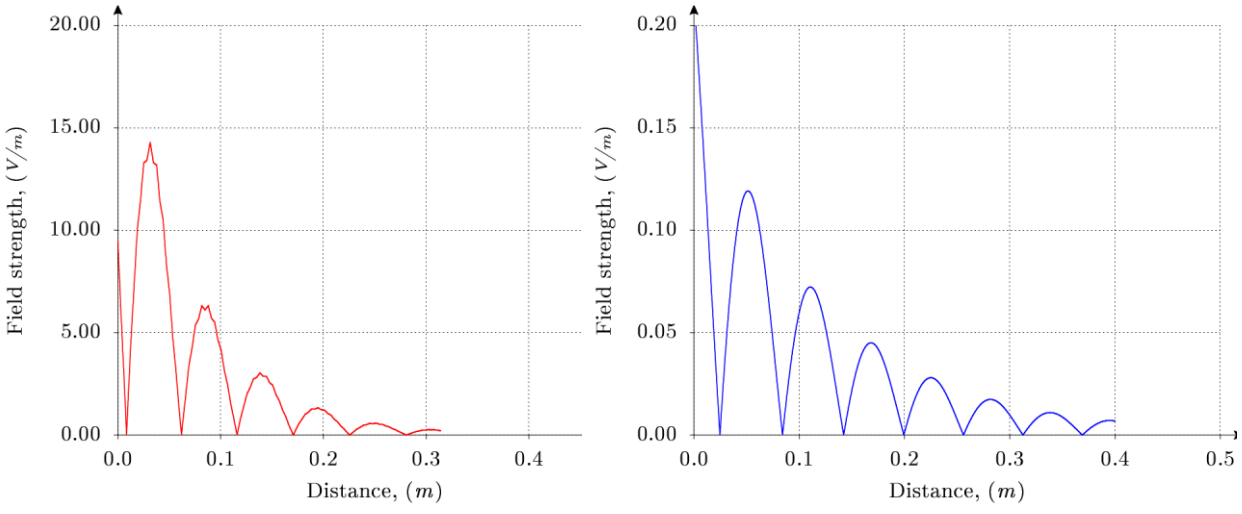

Figure 15. Distribution of the electric component along the computation path at the frequency f = 2.45 GHz: (**a**) the creeping wave (**b**) the surface wave

Typical electric field distribution for the CW and SW along the phantom surface is shown in Figure 15.

Using the simulated field distribution on the phantom surface (Figure 15) one may calculate the wavelength $\lambda = 2l$, where l is the distance between two adjacent minima. The phase velocity is defined as follows:

$$V_{ph} = f \cdot \lambda \,, \tag{12}$$

where f is the frequency of the EM wave propagating along the phantom surface.

The frequency dependence of the phase velocity normalized to the speed of light in the free space for a set of different shoulder radius r is presented in Figure 16. The phantom thickness is $t = 2r$. From the data presented one may conclude, that the CW are characterized by dispersion while the SW are non-dispersive.

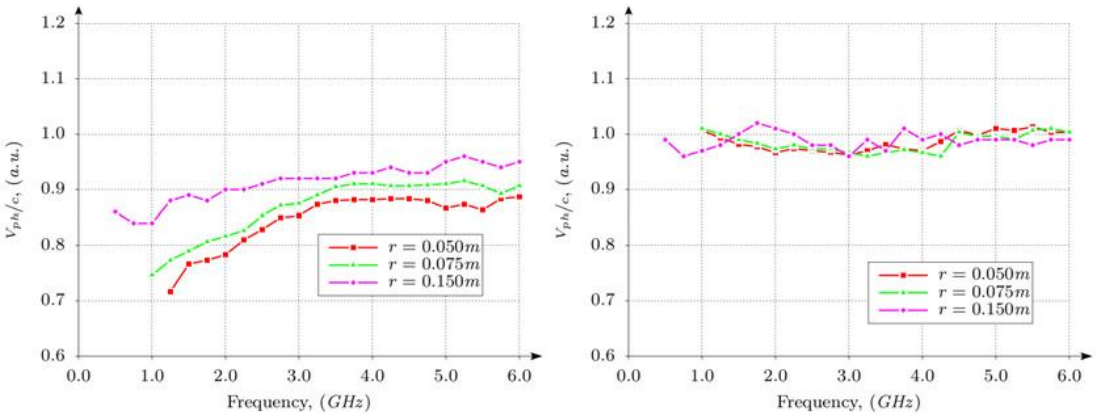

Figure 16. Normalized phase velocity ofwaves for different values of the phantom thickness:(**a**) Creeping; (**b**)Surface.

A simplified analytical model was suggested to calculate the CW phase velocity. Half surface of phantom shoulder with radius R is shown in Figure 17. The phantom shoulder is assumed to be made of a perfect conductor. This assumption is based on a high value of the dielectric constant of the human body at the surface-air interface compared to dielectric permittivity of the air. Arc segment bounded by an angle Θ is chosen to be equal to the half wave length of the creeping wave ($\lambda_{eff}/2$). The length of the tangential segment bounded by the same angle ⊚ is defined as the half wave length of the wave in the free space ($\lambda_0 / 2$).

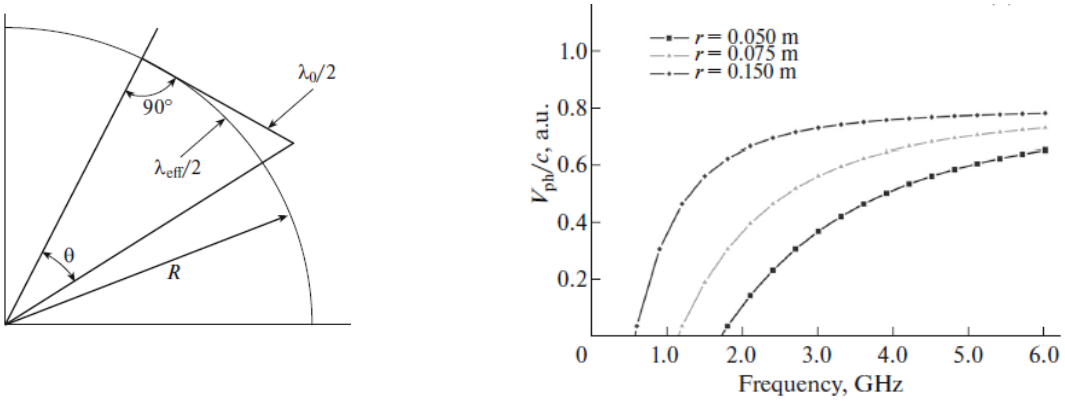

(**a**) (**b**)

Figure 17.(**a**) Simplified geometry of shoulder for creeping wave phase velocity modeling; (**b**)Frequency dependence of normalized phase velocity (simulation results).

Actually, the following inequalities are fulfilled: $\lambda_{eff}<\lambda_0<< R$. In this case, the wavelength of the CW and the wave length in the free space are defined as

$$\frac{\lambda_{eff}}{2} = \Theta \cdot R\,, \tag{13}$$

$$\frac{\lambda_0}{2} = R \cdot \tan\Theta \tag{14}$$

It follows from (13) and (14):

$$\lambda_{eff} = 2 \cdot R \cdot a\tan\left(\frac{\lambda_0}{2 \cdot R}\right) \tag{15}$$

The phase velocity at the frequency f is described by the equation:

$$\frac{v_{eff}}{f} = 2 \cdot R \cdot a\tan\left(\frac{c}{2 \cdot f \cdot R}\right) \tag{16}$$

followed by the normalized effective phase velocity:

$$\frac{v_{eff}}{c} = \frac{2 \cdot f \cdot R}{c} \cdot a\tan\left(\frac{c}{2 \cdot f \cdot R}\right) \tag{17}$$

The frequency dependence of the normalized phase velocity of the CW using (17) is presented in Figure 18 together with results of full-wave simulations.

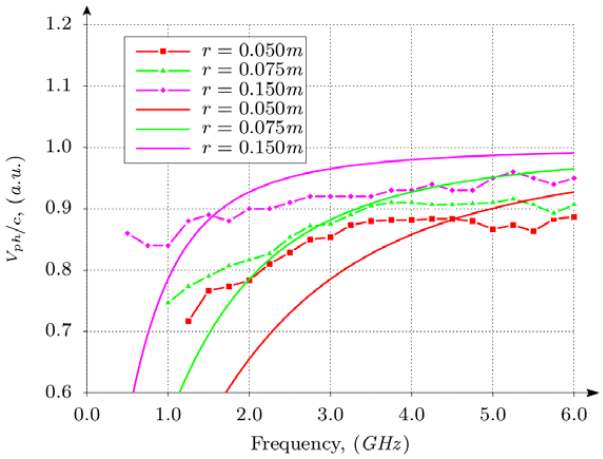

Figure 18. Comparison of analytical model and full wave simulations of creeping wave phase velocity.

Experimental study of the wave propagation over a human body was performed on the volunteer body (Figure 19) to get the most accurate results that are close to realistic phenomena as much as possible. All results were obtained at the frequency f = 2.55 GHz [**Error! Reference source not found.**, **Error! Reference source not found.**-44].

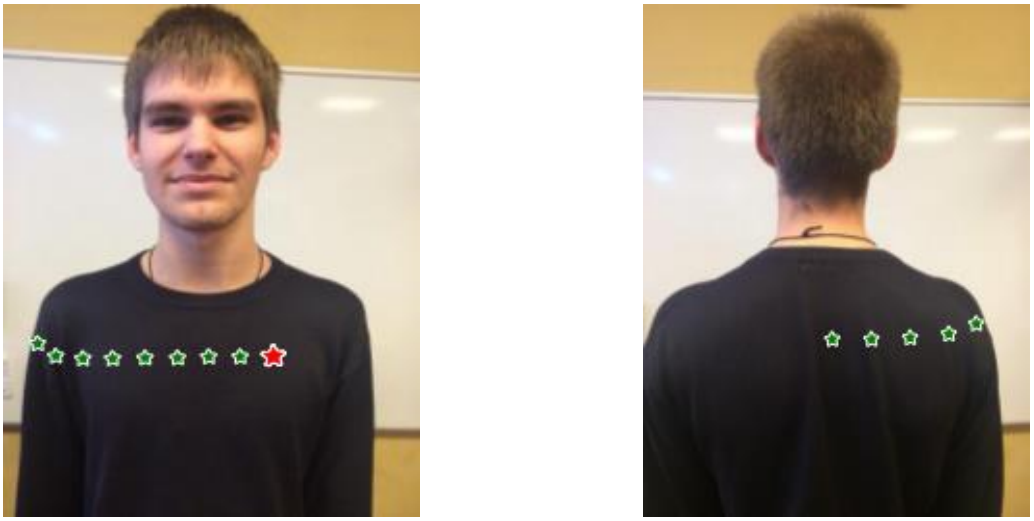

(**a**) (**b**)

Figure 19. Antenna position over the human body. The position of the stationary transmitting antenna is shown by the red star; the green stars show the receiving antenna positions.

Figure 20. Two manufactured disc antennas providing the surface wave excitation.

Two disk antennas presented in Figure 20 were manufactured and tested. Antennas are well matched at the frequency f = 2.55 GHz, which is confirmed by the measurement of the reflection coefficient. The antennas are positioned at height of 5 mm with respect to

the body surface. The experiment was performed by using a Rohde & Schwarz ZVA8 vector network analyzer.

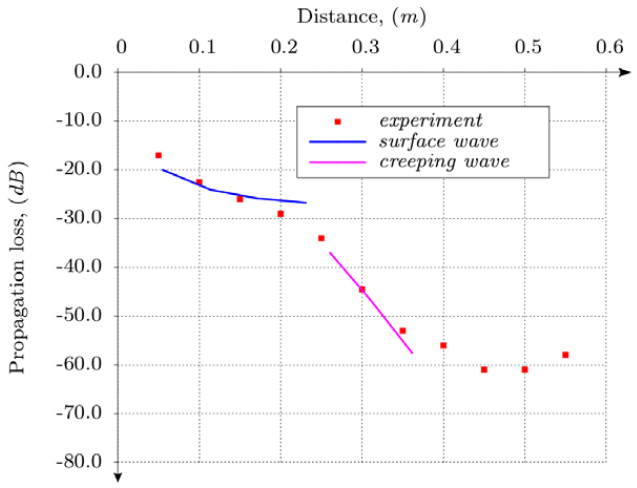

Figure 21. Measured insertion loss between the antennas along the path on body presented in

For attenuation measurements the radiating antenna was placed at the left part of the breast while the receiving antenna was moved along the chest, then around the right shoulder and along the back in the lateral plane as shown in Figure 10. Transmission coefficient (path loss) was measured for each position of the receiving antenna. Measured and simulated results are presented in Figure21. A good agreement is observed between the experimental and numerical results. A couple of experimental points belonging to the back of body do not go well with the modeling results. It could happen because they are influenced by the wave leakage over the shoulder radiated from the transmitting antenna placed on the breast.

Conclusions

The results of theoretical and experimental studies of the propagation of EM waves on the surface of the human body allow drawing the following conclusions:

—A model of a body made of a perfect conductor can be used to simulate the propagation of EM waves in the microwave range using both numerical and analytical methods; the accuracy of the performed calculations is high and suitable for practical applications.

—Analytical and numerical modeling using FDTD allow to calculate accurately the dependence of the propagation losses of EM waves on the distance traveled by the wave and the type of the surface (flat or curved).

—An investigation of the EM wave propagation inside the multilayer biological object demonstrate a possibility to use these waves for microwave diagnostics of the state of different parts of the human body.

—An investigation of the dispersion characteristics of the surface and creeping waves has been carried out; the identified dispersion of the creeping wave should be taken into account in practical applications.

Author Contributions: I.V. – writing: original draft preparation, review and editing the manuscript; O.V. contributed in analytical model development and analysis of EM wave propagaton on the human body surface; V.P. contributed in analysis of EM wave propagation in

multi-layer object and investigation of on-body wave propagation; I.M. investigated the EM wave propagation through the biological medium–air interface; P.T. investigated the EM wave propagation in the regular biological medium and reflection and refraction of the waves on the body-air interface; V. K. took part in all experimental investigations and result analysis.

Funding: This research received no external funding

Acknowledgments: Most of the investigations were supported by theMinistry of Education and Science of the Russian Federation (project no. 8.2579.2014/K).

Conflicts of Interest: The authors declare no conflict of interest.

References

1. K. Finkenzeller, RFID Handbook: Fundamentals and Applications in Contactless Smart Cards, Radio Frequency Identification, and Near-Field Communication, 3rd ed. (Wiley, 2010).
2. J. C. Lin, Electromagnetic Fields in Biological Systems (CRC–Taylor & Francis, London–New York, 2012).
3. P. S. Hall and Y. Hao, Antennas and Propagation for Body-Centric Wireless Communications (Artech House, Norwood, 2012).
4. 4. K. S. Nikita, Handbook of Biomedical Telemetry (Wiley, 2014).
5. E. Moradi, K. Koski, T. Bjorninen, L. Sydanheimo, J. M. Rabaey, J. M. Carmena, Y. Rahmat-Samii, and L. Ukkonen, Miniature implantable and wearable on-body antennas: towards the new era of wireless body-centric systems, IEEE Antennas Propag. Mag. 56, No. 1, 271-291 (2014).
6. R. Paknys, D.R. Jackson, "The Relation Between Creeping Waves, Leaky Waves, and Surface Waves," IEEE Trans. on Antennas and Propag., 2005, vol. 53, № 3, pp. 898 – 907.
7. R. E. Collin, "Field Theory of Guided Waves," McGraw-Hill, New York, 1960.
8. F. Monticone, A. Alu, "Leaky-Wave Theory, Techniques, and Applications: From Microwaves to Visible Frequencies," IEEE Proc., 2015, vol. 103, № 5, pp. 793-821.
9. R. Paknys, N. Wang, "Creeping Wave Propagation Constant and Modal Impedance for Dielectric Coated Cylinder," IEEE Trans. on Antennas and Propag., 1986, vol. 34, № 5, pp. 674 – 680.
10. G.A. Conway, W.G. Scanlon, S.L. Cotton, M.J. Bentum, "An Analytical path-Loss Model for On-Body Radio Propagation," IEEE. URSI Intern Symp. on Electromagnetic Theory, 2010, pp.332
11. Gulich, R.; Köhler, M.; Lunkenheimer, P.; Loidl, A. Dielectric Spectroscopy on Aqueous Electrolytic Solutions. Radiat. Environ. Biophys. 2009, 48, 107–114.
12. C. Kittel, Introduction to Solid State Physics, 5th ed. (Wiley, New York, 1976).
13. Vendik , O. G. Vendik, D. S. Kozlov, I. V. Munina, V. V. Pleskachev, A. S. Rusakov, P. A. Tural'chuk, Wireless monitoring of the biological object state at microwave frequencies: A review, Technical Physics, January 2016, Volume 61, Issue 1, pp 1-22
14. C. Gabriel, S. Gabriel, and E. Corthout, The dielectric properties of biological tissues: I. Literature survey, Physics in Medicine and Biology, vol. 41, no. 11, pp. 2231–2249, 1996.
15. S. Gabriel, R. W. Lau, and C. Gabriel, The dielectric properties of biological tissues: II. Measurements in the frequency range 10Hz to 20GHz, Physics in Medicine and Biology, vol. 41, no. 11, pp. 2251–2269, 1996.
16. PA Hasgall, F Di Gennaro, C Baumgartner, E Neufeld, MC Gosselin, D Payne, AKlingenbock, and N Kuster. IT'IS Database for thermal and electromagnetic parameters of biological tissues. Version 2.6, January 13th. 2015, 2015.
17. Maria A. Stuchly, T. Whit Athey, George M. Samaras, and Glen Edward Taylor, "Measurement of Radio Frequency Permittivity of Biological Tissues with an Open-Ended Coaxial Line: Part II—Experimental Results", IEEE 'Trans. on MTT", V. 30, no. 1, pp. 87-92, 1982.
18. A. Tural'chuk, O. G. Vendik, and I. B. Vendik, «Propagation of Electromagnetic Waves in Biological Media: Refraction at Interfaces», Technical Physics Letters, 2015, Vol. 41, No. 3, pp. 270–272
19. P. Turalchuk, I. Munina, M. Derkach, O. Vendik, and I. Vendik, "Electrically Small Loop Antennas for RFID Applications", IEEE Antennas and Wireless Propagation Letters, Vol.14, Issue 1, 17 April PL-02-15-0349)
20. E. Kunakovskaya, I. Munina, P. Turalchuk, I. Vendik, M. Derkach, Propagation of Electromagnetic Waves through. Interface of Biological Tissue and Free Space, 2016 Loughborough Antennas & Propagation Conference, 14 - 15 November 2016, p

21. Irina Munina, PavelTuralchuk, Ekaterina Kunakovskaya, Irina Vendik, Attenuation of electromagnetic waves radiated by an implanted antenna, Proceedings of the International Conference "Days on Diffraction", June 27 - July 1, 2016, St. Petersburg, Russia, pp. 309-313
22. P. Turalchuk, I. Munina, M. Derkach, O. Vendik, and I. Vendik, "Propagation of Electromagnetic Waves Radiated by an Implanted Antenna", Proc. of 45thEuropean Microwave Conference, Paris, France, 6-11 September, 2015, pp. 387-390.
23. C. A. Balanis, Antenna Theory: Analysis and Design, New York: Wiley, 2005, p. 1136.
24. SEMCAD X by SPEAG, www.semcad.com
25. D. M. Hagl, D. Popovic, S. C. Hagness, J. H. Booske, and M. Okoniewski, "Sensing volume of open-ended coaxial probes for dielectric characterization of breast tissue at microwave frequencies," IEEE Transactions on Microwave Theory and Techniques, vol. 51, no. 4 I, pp. 1194–1206, 2003.
26. M. Lazebnik, D. Popovic, L. McCartney et al., "A large-scale study of the ultrawideband microwave dielectric properties of normal, benign and malignant breast tissues obtained from cancer surgeries," Physics in Medicine and Biology, vol. 52, no. 20, pp. 6093–6115, 2007.
27. K. R. Foster, J. L. Schepps, R. D. Stoy, and H. P. Schwan, "Dielectric properties of brain tissue between 0.01 and 10 GHz," Physics in Medicine and Biology, vol. 24, no. 6, pp. 1177–1187, 1979.
28. Mohammed B. J., Abbosh, A. M., Mustafa, S., et al. Microwave system for head imaging. IEEE Trans. on Instrumentation and Measurement, Vol. 63, No. 1, January 2014, p. 117-123
29. E. Moradi, K. Koski, T. Bjorninen, L. Sydanheimo, J. M. Rabaey, J. M. Carmena, Y. Rahmat-Samii, and L. Ukkonen, "Miniature implantable and wearable on-body antenns: towards the new era of wireless body-centric systems, IEEE Antennas Propag. Mag. 56, 1, 271-291, (2014).
30. Meaney P.M. 3D Micowave bone imaging. Conf. Proc. 6th European Conference on Antennas and Propagation (EUCAP) 2011. doi: 10.1109/EuCAP.2012.6206024.
31. Paul M. Meaney, Tian Zhou, Douglas Goodwin, Amir Golnabi, Elia A. Attardo, and Keith D. Paulsen, Bone Dielectric Property Variation as a Function of Mineralization at Microwave Frequencies, Hindawi Publishing Corporation International Journal of Biomedical Imaging, vol.7, 2012, Article ID 649612, 9 pages doi:10.1155/2012/649612C.
32. Irina Vendik, Vladimir Pleskachev, Viktor Yakovlev, Svetlana Tamilova, Microwave diagnostics of osteoporosis, 2018 IEEE Conference of Russian Young Researchers in Electrical and Electronic Engineering (2018 ElConRus), St. Petersburg, February 2018, c. 319-325
33. Irina B. Vendik, Mikhail A. Odit, Vitali V. Kirillov, Svetlana Tamilova, Viktor A. Yakovlev, Konstantin Zolototrubov, Vladimir. V. Pleskachev, Diagnostic of osteoporosis based on analysis of electromagnetic wave propagation in biological objects, Conference: 2019 Antennas Design and Measurement International Conference ADMiNC 2019, October 2019, DOI: 10.1109/ADMInC47948.2019.8969252
34. Sergey N. Makarov, William Appleyard, Patrick D. Carberry, Harshal V. Tankaria1, Gregory M. Noetscher1, AraNazarian, Novel On-Body Microwave Antenna Array Testbed for Highly-Sensitive Measurements of Wrist Bone Signature, IEEE, AP-S 2017, pp. 1231-1232.
35. Bilal Amin, AtifShahzad, Laura Farina, Eoin Parle, Laoise McNamara, Martin O'Halloran, MuhammadAdnanElahi, Dielectric characterization of diseased human trabecular bones at microwave frequency, Medical Engineering and Physics 78 (2020) 21–28
36. J. S. Bobowski and T. Johnson, Permittivity measurements of biological samples by an open-ended coaxial line, Progress In Electromagnetics Research B, Vol. 40, pp.159-183, 2012
37. R. Zajíček, J. Vrba, K. Novotný, Evaluation of a Reflection Method on an Open-Ended Coaxial Line and its Use in Dielectric Measurements, ActaPolytechnica, Vol. 46 No. 5/2006 pp. 50-54
38. Alessandra La Gioia, Emily Porter, IljaMerunka, AtifShahzad, SaqibSalahuddin, Marggie Jones and Martin O'Halloran, Open-Ended Coaxial Probe Technique for Dielectric Measurement of Biological Tissues: Challenges and Common Practices Review Diagnostics 2018, 8, 40; doi:10.3390/diagnostics8020040 38 p.
39. Dassault Systems. https://www.3ds.com/products-services/simulia/products/cst-studio-suite/ (archived on 24 April 2021).
40. T. Mavridis, L. Petrillo, J. Sarrazin, D. Lautru, A. Benlarbi-Delai, et al. "Creeping Wave Model of Diffraction of an Obliquely Incident Plane Wave by a Circular Cylinder at 60 GHz, IEEE Trans. on Antennas and Propagation. 2014. Vol. 62. № 3, pp. 1372 – 1377.
41. I.V. Andronov and D. Bouche, Electromagnetic Creeping Waves and their degeneration, // - PIERS Proc. 2009, Aug. 18-21. - pp. 1518-1521
42. Vladimir Pleskachev, Irina Vendik, OrestVendik, VitalyKirillov, PavelTuralchuk, Mikhail Odit, On-Body Surface Electromagnetic Wave Propagation: Modeling and Measurements, EuCAP 2016, 11-15 April 2016, Davos, Switzerland, 5 p
43. I.B. Vendik, O. G. Vendik, V. V. Kirillov, V. V. Pleskachev, and P. A. Tural'chuk, Modeling the Propagation of Electromagnetic Waves over the Surface of the Human Body, Technical Physics, 2016, Vol. 61, No. 12, pp. 1765–1775.

44. VitalyKirillov and Irina Vendik, Propagation of electromagnetic waves along the surface of biological objects, 2016 IEEE NW Russia Young Researchers in Electrical and Electronic Engineering Conference (EIConRusNW), St. Petersburg, Russia, February 2016, pp. 764-766, DOI:10.1109/EIConRusNW.2016.7448293